

# An Informatics Approach Identifying Markers of Chemosensitivity in Human Cancer Cell Lines<sup>1</sup>

Sally A. Amundson<sup>2</sup>, Timothy G. Myers,<sup>3</sup> Dominic Scudiero, Shinichi Kitada, John C. Reed, and Albert J. Fornace, Jr.

NIH, National Cancer Institute, Biological Research Laboratory [S. A. A., A. J. F.] and Developmental Therapeutics Program [T. G. M.], Bethesda, Maryland 20892; Frederick Cancer Research Facility, Frederick, Maryland 21702 [D. S.]; and The Burnham Institute, La Jolla, California 92037 [S. K., J. C. R.]

## ABSTRACT

We have used a sensitive and reproducible method of measuring mRNA expression to compare basal levels of 10 transcripts in the 60 cell lines of the National Cancer Institute's *in vitro* anticancer drug screen (NCI-ACDS) under conditions of exponential growth. The strongest correlation among these target genes was between levels of *CIP1/WAF1* and *BAX*. Levels of the three major growth arrest and DNA damage-inducible gene transcripts, (*GADD34*, *GADD45*, and *GADD153*), which are coordinately regulated in response to many stresses, were also correlated across the 60 cell lines. Although the stress induction of several of the transcripts studied here has been shown to be dependent on wild-type p53 status, basal levels of only *CIP1/WAF1* and *BAX* were found to correlate with p53 status. As expected, basal expression of *O*<sup>6</sup> alkyl guanine alkyl-transferase correlated well with resistance to *O*<sup>6</sup>-alkylating agents ( $r = -0.44$ ) but not with resistance to alkylators with different mechanisms of action ( $r = -0.04$ ). When basal expression levels of the 10 genes across the NCI-ACDS panel were compared with sensitivities to a panel of 122 standard chemotherapy agents, the most striking relationship was a strong negative correlation ( $r = -0.3$ ) between basal *BCL-X* levels and sensitivity to drugs in all of the mechanistic classes except one class of antimetabolites. Sensitivities to a maximally diverse sample of 1200 from 70,000 compounds tested in the NCI-ACDS of agents were also negatively correlated with *BCL-X* levels. A novel application of factor analysis revealed that the newly discovered associations were independent of previously demonstrated sensitivity factors such as p53 mutation status and native population doubling time. A similar pattern of correlation was seen for Bcl-X<sub>L</sub> protein levels. Conversely, *BAX* and *BCL2*, two other genes associated with regulation of apoptosis, showed no overall correlation with drug sensitivities. This suggests that *BCL-X* may play a unique role in general resistance to cytotoxic agents, with the cell lines demonstrating relative resistance to 70,000 cytotoxic agents in the NCI-ACDS being characterized by high *BCL-X* expression.

## INTRODUCTION

The NCI-ACDS<sup>4</sup> panel (1, 2) consists of 60 cell lines selected from human tumors of different tissues of origin (breast, central nervous system, colon, bone marrow, lung, skin, ovary, prostate, and kidney). Nearly 100,000 chemical compounds have been tested for cytotoxicity in this panel using a 2-day assay to determine the GI<sub>50</sub> in each cell line (1), with more compounds being tested continually. In addition to identification of potential antineoplastic drugs, these 60 cell lines are also being characterized on a molecular level to define alterations in genes that may contribute to carcinogenesis. Appropriate data mining of such databases may in turn aid in the development of compounds

with specific cytotoxicity directed against cancer cells with particular molecular characteristics (3).

Although expression at the protein level (4) may be a more accurate predictor of activity in the cell, mRNA expression can be a very useful end point for comparison between cell lines. When mRNA levels are informative, their measurement would have the practical advantage of requiring a relatively small sample as well as being more quantitative, rapid, and sensitive. It is also possible to use RNA analysis for newly identified target genes in advance of antibody availability. Microarray technologies promise to yield quantitative measurement of thousands of mRNA levels at once (5, 6), which paves the way for such applications as molecular tumor profiling and precise tailoring of individual chemotherapy regimens.

Accurate measurements of relative basal mRNA levels in human cancer cell lines may provide insight into mechanisms of molecular regulation, interactions, and drug action when this information is considered in the context of the other data in the NCI-ACDS. For instance, our laboratory recently identified a subset of the p53 wild-type cell lines with reduced or absent induction of *GADD45* after  $\gamma$ -irradiation (7). When the NCI-ACDS database was searched for differential sensitivity of this subset of cell lines to cytotoxic drugs, topoisomerase II inhibitors were found to be significantly less toxic in the cell lines with defective *GADD45* induction ( $P < 0.0001$ ). This difference was confirmed by the demonstration that etoposide 16 toxicity and DNA-protein cross-links were decreased when *GADD45* expression was blocked with an antisense vector and led to discovery of a role for Gadd45 in regulating chromatin accessibility (8). This example demonstrates how mechanistic insight can be gained by exploring hypotheses suggested from analysis of a large, complex, but well-controlled biological survey.

We have performed a careful quantitation of the relative basal levels of 10 transcripts chosen for their known roles in cellular damage responses or cancer biology and as potential modifiers of toxicity (*O6AT*, *CIP1/WAF1*, *GADD34*, *GADD45*, *GADD153*, *cMYC*, *MDM2*, *BAX*, *BCL2*, and *BCL-X<sub>L</sub>*) in the 60 cell lines of the NCI-ACDS and looked for correlations between levels of these transcripts, p53 status, and cytotoxicity of the tested compounds in the NCI-ACDS database. Many statistically significant and interesting associations with existing molecular target profiles were observed. In this report, we highlight those we found most provocative, but other correlations can be explored.<sup>5</sup> One of the most striking findings in the present study was the overall negative correlation between *BCL-X* levels and sensitivity to the 122 "standard" chemotherapy agents with the exception of one group of antimetabolites. This correlation was stronger than the positive correlation with cytotoxicity previously reported for p53 across diverse mechanisms of drug action (9) and suggests the importance of endogenous *BCL-X* levels in the cellular response to chemotherapeutic agents, independent of p53 status.

Received 2/25/00; accepted 8/24/00.

The costs of publication of this article were defrayed in part by the payment of page charges. This article must therefore be hereby marked *advertisement* in accordance with 18 U.S.C. Section 1734 solely to indicate this fact.

<sup>1</sup> Supported in part by NIH Grants GM60554 and CA78040 (to J. C. R. and S. K.).

<sup>2</sup> To whom requests for reprints should be addressed, at NIH, National Cancer Institute, 37 Convent Drive, Building 37, Room 5C09, Bethesda, MD 20892.

<sup>3</sup> Present address: Large Scale Proteomics Corp., Rockville, MD 20850.

<sup>4</sup> The abbreviations used are: NCI-ACDS, National Cancer Institute's anticancer drug screen; GI<sub>50</sub>, 50% growth-inhibitory concentration; GADD, growth arrest and DNA damage-inducible; poly(A), polyadenylate; PCNU, 1-(2-chloroethyl)3-(2,6-dioxo-3-piperidyl)-1-nitrosourea.

<sup>5</sup> Internet address to access the NCI-ACDS database and the NCI Developmental Therapeutics Program: <http://dtp.nci.nih.gov/>.

## MATERIALS AND METHODS

**Cell Culture.** Cells from the NCI-ACDS cancer cell panel (9) were grown in RPMI 1640 supplemented with 10% fetal bovine serum and 100 units/ml penicillin (Sigma) and 100  $\mu\text{g/ml}$  streptomycin (Sigma). All of the cultures were maintained at 37°C in a humidified 5% CO<sub>2</sub> atmosphere. Cells were lysed for RNA harvest at 40–60% confluence. Suspension cell lines were maintained between 1 and 10  $\times 10^5$  cells/ml and were harvested in log phase growth at 4–5  $\times 10^5$  cells/ml. All of the cultures were fed with fresh medium the day before harvest.

**Quantitative Expression Analysis.** mRNA was isolated by the guanidine thiocyanate method of Chomczynski and Sacchi (10), followed by poly(A) purification using oligodeoxythymidylate cellulose as previously described (11). cDNA probes for *GADD34*, *GADD45*, and *GADD153* were obtained by excising the insert from pHu34B (12), pHu45 (12), and pHu75 (13), respectively. Other cDNA plasmids were obtained from Oncor (*c-MYC*) or were generously provided by B. Vogelstein of The Johns Hopkins University, Baltimore, MD (*MDM2*), S. Korsmeyer of the Washington University School of Medicine, St. Louis, MO (*BAX* and *BCL2*), W. El-Deiry of the University of Pennsylvania School of Medicine, Philadelphia, PA (*CIP1/WAF1*), and L. Boise of the University of Miami School of Medicine, Miami, FL (*BCL-X*). The cDNA inserts were labeled with <sup>32</sup>P using the PrimeIt RT system (Stratagene) according to the directions of the supplier. Twofold serial dilutions of the mRNAs were fixed on nylon membranes, with six copies of each filter being made from the same RNA dilution at one time. For each transcript, hybridization to the labeled cDNA probe was carried out on a complete filter set (which included RNA samples from all of the cell lines in the screen) in the same hybridization mix. High-stringency hybridization and wash conditions were as previously described (11). Hybridization was quantitated on a phosphorimager (Molecular Dynamics). Relative signal levels, normalized to the poly(A) content of each sample, were determined using the RNA Analysis program as previously described (14). Relative protein levels of Bcl-X<sub>L</sub> and Bax were measured using standard Western blotting techniques as previously described (15).

**Statistical Methods.** Growth inhibition patterns (IC<sub>50</sub> values for 60 human tumor cell lines) were those available from the NCI Developmental Therapeutics Program.<sup>5</sup> Values were reexpressed as potency values by using the negative log of the molar concentration calculated in the NCI screen. The dependence of drug potency on gene expression levels was gauged using either the Spearman correlation coefficient for continuous value gene expression measurements, such as *GADD45* expression, or the Wilcoxon Rank Sum test for binary gene expression measurements, such as Mer<sup>-</sup>/Mer<sup>+</sup> or p53 wild-type/mutant. Positive correlations occurred when relatively high levels of gene expression were found in relatively sensitive cell lines. Negative correlations occurred when relatively high levels of gene expression were found in resistant cell lines.

Partial correlations were calculated using SAS Proc Corr (SAS Institute, Cary, NC); *e.g.*, to find the residual correlation between chemosensitivity and *BCL-X* after “removing” any contributions attributable to a correlation between chemosensitivity and measured doubling time, Proc Corr was executed with drug potency and *BCL-X* levels listed as the variables to test correlation and with doubling time listed as the partial variable. In this way, the potential role of previously demonstrated sensitivity factors (“molecular targets”) as underlying factors responsible for the present observed correlations could be examined statistically.

To visualize a large number of correlation or Wilcoxon test results simultaneously, we first calculated the asymptotic *P* from the test statistic for each test using normal approximation and then plotted the results for all of the tests in a histogram or color-coded table. The histogram reveals the number of drug sensitivity correlations that would have been considered statistically significant had each drug’s correlation with gene expression been evaluated alone. The same histogram can reveal positive or negative trends that might not have been detected by a simple count of individual results above a particular significance threshold. The colorized matrix (or in some cases a single column) of *P* also highlights the statistical significance of correlation test results as well as positive or negative trends but allows the display of results according to a logical (drug mechanism of action) or empirical (cluster) order.

The *P* reported here correspond to the single-tailed test, in which the alternative hypothesis is that the correlation is negative and the null hypothesis

is that the correlation is zero. As such, a significant negative correlation ( $\alpha = 0.05$ ) will be reported on our one-sided *P* scale as 0.05, whereas a significant positive correlation ( $\alpha = 0.05$ ) will be reported as 0.95. The latter case can be understood as there being a 95% probability of finding a more negative correlation by chance, whereas more positive correlations happen because of chance alone only 5% of the time, indicating with reasonable certainty that the correlation is positive.

**Unidrug Pattern Data Set.** To reduce the bias in the drug screen database toward the overrepresentation of some chemical structure and activity classes, a k-means, algorithm-based clustering process was developed.<sup>6</sup> A series of iterative clustering optimizations was performed on the NCI-ACDS IC<sub>50</sub> patterns to find 1200 clusters that were well populated but maximally diverse in pattern. Exemplar compounds, nonconfidential compounds closest to the center of each cluster, were taken to represent the entire database. In theory and as first demonstrated by early applications of the COMPARE program<sup>7</sup> and many examples since, highly correlated groups of compounds will share the same physicochemical properties and more importantly, often share mechanism of action properties. This phenomenon was named by the late Ken Paull the “COMPARE effect.” Appropriately, the sets of compounds represented by the database exemplars are termed compare effect clusters. When a molecular target pattern comprising some cell characteristic measured in the NCI-ACDS is used to search for correlating activity patterns, a search against the redundancy-reduced set of compare effect cluster exemplars is expected to provide a more concise and accurate survey of the molecular target’s role in measured cytotoxicity.

## RESULTS

**Accurate Measurement of Basal mRNA Levels.** Many of the transcripts measured in this study previously have been shown to be induced by alteration in growth conditions, including confluence and starvation stress (16–20), so maintaining consistent growth conditions was crucial for meaningful and reproducible measurement of basal RNA levels. Culture conditions were especially important in lymphoid and myeloid lines, a point that is often overlooked as the concept of confluence does not apply to such cell lines. For instance, when the lymphoid cell line Molt4 was deliberately grown past exponential growth phase without the addition of fresh medium, *GADD45*, *CIP1/WAF1*, and *MDM2* were all induced 10-fold or more over the levels present several days previously in the same culture while in exponential growth (data not shown). In the same experiment, however, no change was found in the levels of *GADD34*, *GADD153*, *BAX*, *BCL-X<sub>L</sub>*, *cMYC*, or *O6AT*. To avoid the potential confounding effects of starvation, glucose deprivation, or other overgrowth-related stresses in various cell lines, all of the cultures were maintained in exponential growth, with suspension lines kept at densities of 2–10  $\times 10^5$  cells/ml. All of the cell lines were fed with fresh medium the day before harvest of RNA. Attached cell lines were harvested at 40–60% confluence, whereas suspension lines were harvested at densities of 4–5  $\times 10^5$  cells/ml.

In previous studies with inducible genes (21–23) our laboratory has developed an accurate and rapid approach for comparative measurements of low-abundance transcripts (11) that is less labor intensive than RNase protection and that avoids the problems of normalization inherent in Northern blot analysis of weakly expressed transcripts. Serial dilutions of poly(A) RNA are hybridized to a radioactive probe and used to generate a standard calibration curve. This compensates for the nonlinearity (pseudo-first-order kinetics) of signal to mRNA content, which can be encountered in hybridizations, such as when the probe is not in excess (11, 24). Replicate membranes made with the same serially diluted RNA samples are hybridized to a polyuridylic acid probe to control for differences in the poly(A) RNA content between different samples or for any loading differences between lanes. The poly(A) content of different samples is

<sup>6</sup> T. G. Myers, unpublished results. Details are available at <http://www.chemoddb.org>.

<sup>7</sup> Written by K. Paull in the DTP of the NCI. Details are available at <http://dtp.nci.nih.gov/docs/compare/compare.html>.

generally within ~25%, although greater variations did sometimes occur between different cell lines. Hybridization to a polyuridylic acid probe effectively corrects for such variations (14). This method is also much more reliable than normalization to so-called housekeeping genes, such as *GAPDH* or  $\beta$ -actin, which can show considerable variability between different cell lines. Overall, this technique has been shown to yield accurate determinations of low-abundance transcripts (on the order of  $1/10^5$ ) and to reliably detect differences of 1.5-fold or greater (11, 14, 25) with results comparable with those of RNase protection (26). Such sensitivity and accuracy are critical for the meaningful comparison of uninduced basal levels of transcripts in different cell lines and exceed the

degree of accuracy possible for measurements of relative protein levels or for many other methods of measuring relative mRNA levels, including most array applications. Using this approach, we determined the relative basal levels of the mRNAs for the genes *GADD34*, *GADD45*, *GADD153*, *BAX*, *BCL2*, *BCL-X<sub>L</sub>*, *MDM2*, *CIP1/WAF1*, *O6AT*, and *cMYC* in the 60 human cancer cell lines of the NCI-ACDS. RNA samples from all of the 60 cell lines were hybridized together at high stringency in the same hybridization mix at the same time to avoid variations in hybridization conditions. The results of quantitative hybridization of these 10 transcripts are presented in Table 1 as basal levels relative to the levels in BT549 or in the case of *BCL2*, which was not detectable in this cell line,

Table 1 Relative basal mRNA and protein levels in cell lines of the NCI-ACDS

| Cell line | Type <sup>a</sup> | <i>c-MYC</i> <sup>b</sup> | <i>GADD45</i> | <i>O6AT</i> | <i>BAX</i> | <i>MDM2</i> | <i>WAF-1</i> | <i>GADD153</i> | <i>GADD34</i> | <i>BCL-X</i> | <i>BCL2</i> <sup>c</sup> | <i>BAX</i> <sup>d</sup> | <i>BCL-XL</i> <sup>d</sup> |
|-----------|-------------------|---------------------------|---------------|-------------|------------|-------------|--------------|----------------|---------------|--------------|--------------------------|-------------------------|----------------------------|
| BT549     | Breast            | 1                         | 1             | 1           | 1          | 1           | 1            | 1              | 1             | 1            | 0                        | 1                       | 1                          |
| HS578T    | Breast            | 0.37                      | 2.15          | 0           | 0.57       | 0.66        | 1.73         | 0.84           | 2.23          | 0.7          | 0                        | 0.7                     | 0.7                        |
| MCF7      | Breast            | 0.41                      | 0.18          | 2.27        | 0.26       | 0.41        | 0.91         | 0.46           | 0.16          | 0.26         | 5.1                      | 0.9                     | 1.2                        |
| MDA-MB231 | Breast            | 0.62                      | 0.63          | 0           | 0.83       | 0.59        | 1.77         | 0.69           | 1.7           | 3.58         | 3.9                      | 1.3                     | 1.5                        |
| MDA-MB435 | Breast            | 0.73                      | 0.15          | 0           | 0.24       | 0.45        | 0.49         | 0.61           | 0.88          | 0.37         | 1.3                      | 1.1                     | 0.2                        |
| MDA-N     | Breast            | 0.47                      | 0.26          | 0           | 0.14       | 0.32        | 0.18         | 0.89           | 0.76          | 0.18         | 1                        | 0.9                     | 0.7                        |
| NCI-ADR   | Unknown           | 0.8                       | 1.45          | 0.91        | 0.4        | 1.41        | 1.23         | 0.69           | 1.06          | 0.6          | 0                        | 0.9                     | 0.9                        |
| T47D      | Breast            | 0.38                      | 0.12          | 2.1         | 0.19       | 0.76        | 2.19         | 0.89           | 0.24          | 1.32         | 0.4                      | 0.7                     | 1.6                        |
| SF-268    | CNS <sup>e</sup>  | 0.44                      | 2.76          | 0           | 0.43       | 0.58        | 0.48         | 1.53           | 2.27          | 0.67         | 0                        | 1.6                     | 1.2                        |
| SF-295    | CNS               | 0.2                       | 0.52          | 0.09        | 0.42       | 0.26        | 1.33         | 0.74           | 1.31          | 0.34         | 0                        | 1.1                     | 0.4                        |
| SF-539    | CNS               | 0.3                       | 1.55          | 0           | 0.39       | 0.58        | 1.3          | 0.74           | 1.37          | 0.54         | 0.9                      | 0.6                     | 0.2                        |
| SNB19     | CNS               | 0.3                       | 0.7           | 0           | 0.41       | 0.55        | 1.63         | 0.41           | 0.78          | 0.92         | 0                        | 1                       | 1                          |
| SNB75     | CNS               | 0.22                      | 0.78          | 0           | 0.45       | 0.52        | 1.18         | 0.43           | 1.11          | 0.33         | 0                        | 1.4                     | 0.2                        |
| U251      | CNS               | 0.21                      | 0.63          | 0           | 0.24       | 0.52        | 0.88         | 1.02           | 0.44          | 0.29         | 0                        | 1                       | 0.2                        |
| COLO205   | Colon             | 0.77                      | 0.6           | 3.8         | 0.52       | 0.44        | 0.97         | 1.72           | 0.59          | 1.5          | 0.1                      | 1.4                     | 0.5                        |
| HCC-2998  | Colon             | 0.67                      | 0.64          | 2.13        | 0.36       | 0.53        | 1.02         | 1.21           | 0.83          | 0.75         | 0.1                      | 0.9                     | 0.7                        |
| HCT116    | Colon             | 1.92                      | 1.15          | 0.75        | 0.4        | 0.44        | 2.96         | 0.61           | 0.74          | 1.03         | 0.2                      | 0.6                     | 1.2                        |
| HCT15     | Colon             | 0.37                      | 0.42          | 2.2         | 0.63       | 0.36        | 0.84         | 0.45           | 0.83          | 0.76         | 0.2                      | 1.6                     | 1.1                        |
| HT29      | Colon             | 0.78                      | 0.61          | 1.52        | 0.43       | 0.26        | 1.06         | 1.2            | 0.78          | 1.05         | 0.1                      | 0.9                     | 1.4                        |
| KM12      | Colon             | 0.83                      | 0.79          | 0           | 0.19       | 0.36        | 0.27         | 0.77           | 0.7           | 0.68         | 0.3                      | 0                       | 0.2                        |
| SW620     | Colon             | 1                         | 1.26          | 0           | 0.24       | 1.08        | 0.19         | 0.4            | 0.26          | 1.02         | 0.6                      | 1                       | 1.6                        |
| A549      | Lung              | 0.75                      | 0.52          | 0.61        | 1.12       | 0.58        | 3.11         | 0.37           | 0.76          | 1.82         | 0.4                      | 1.1                     | 1.4                        |
| EKVX      | Lung              | 0.48                      | 0.72          | 2.04        | 0.41       | 0.66        | 0.66         | 0.56           | 0.64          | 0.9          | 0.7                      | 1                       | 1                          |
| HOP62     | Lung              | 0.4                       | 1.61          | 0.58        | 0.22       | 0.5         | 1.27         | 1.31           | 0.7           | 0.75         | 0.2                      | 0.8                     | 1.4                        |
| HOP92     | Lung              | 1.12                      | 2.44          | 0           | 1.97       | 0.9         | 6.75         | 1.35           | 1.55          | 1.57         | 0.7                      | 0.9                     | 1.6                        |
| NCI-H226  | Lung              | 1.14                      | 9.47          | 0           | 1.25       | 2.43        | 12.94        | 3.12           | 2.39          | 1.53         | 2.2                      | 1.4                     | 1.4                        |
| NCI-H23   | Lung              | 0.92                      | 0.91          | 2.1         | 0.72       | 0.7         | 2.53         | 1.31           | 0.58          | 0.5          | 0.2                      | 0.9                     | 0.6                        |
| NCI-H322M | Lung              | 0.46                      | 1.37          | 0.23        | 0.29       | 0.97        | 2.84         | 1.26           | 1.16          | 1.55         | 1.8                      | 0.8                     | 1.2                        |
| NCI-H460  | Lung              | 1.54                      | 0.61          | 0.97        | 0.49       | 0.37        | 4.02         | 0.34           | 0.25          | 0.4          | 3                        | 0.1                     | 0.2                        |
| NCI-H522  | Lung              | 1.2                       | 0.45          | 1.8         | 0.51       | 0.94        | 2.57         | 0.73           | 0.52          | 0.46         | 0.9                      | 0.3                     | 0.8                        |
| CCRF-CEM  | Lymphoid          | 1.42                      | 0.27          | 2.14        | 0.35       | 0.85        | 0.07         | 0.65           | 0.21          | 0.48         | 0.8                      | 1.1                     | 1.2                        |
| HL60      | Lymphoid          | 3.31                      | 0.32          | 1.03        | 0.25       | 0.36        | 0.12         | 1.33           | 0.42          | 0.04         | 1.8                      | 0.8                     | 0.2                        |
| K562      | Lymphoid          | 1.19                      | 2.1           | 0           | 0.32       | 0.36        | 0.5          | 2.29           | 1.04          | 0.88         | 0.2                      | 0.8                     | 1.6                        |
| MOLT4     | Lymphoid          | 0.95                      | 0.4           | 1.35        | 0.49       | 1.01        | 0.15         | 4.32           | 0.68          | 0.81         | 2.7                      | 1.1                     | 0.7                        |
| RPMI 8226 | Lymphoid          | 3.76                      | 1.17          | 0.4         | 0.25       | 0.85        | 0.48         | 0.3            | 0.13          | 0.57         | 5.3                      | 0.8                     | 0.4                        |
| SR        | Lymphoid          | 0.67                      | 1.08          | 0           | 0.74       | 0.73        | 3.39         | 0.65           | 0.57          | 0.19         | 0.6                      | 1.6                     | 0.2                        |
| LOX-IVMI  | Melanoma          | 1.82                      | 2.13          | 0           | 1.11       | 0.47        | 5.6          | 0.71           | 2.29          | 0.49         | 1.5                      | 0.9                     | 0.7                        |
| M14       | Melanoma          | 0.84                      | 0.46          | 2.13        | 0.53       | 1           | 1.59         | 0.55           | 1.5           | 0.29         | 2                        | 1                       | 0.3                        |
| MALME-3M  | Melanoma          | 0.22                      | 0.72          | 0.38        | 0.41       | 0.84        | 3.93         | 1.66           | 0.77          | 0.45         | 0.7                      | 1.3                     | 0.2                        |
| SK MEL2   | Melanoma          | 0.39                      | 0.55          | 0.9         | 0.29       | 0.53        | 0.29         | 0.96           | 1.4           | 0.24         | 4.9                      | 1.1                     | 1.5                        |
| SK MEL28  | Melanoma          | 0.43                      | 1.11          | 0.98        | 0.78       | 0.6         | 0.52         | 0.56           | 1.36          | 0.38         | 1.5                      | 1.4                     | 0.1                        |
| SK-MEL5   | Melanoma          | 0.54                      | 0.46          | 0.37        | 0.6        | 0.47        | 1.8          | 0.75           | 0.32          | 0.22         | 0.6                      | 1.2                     | 0.7                        |
| UACC-257  | Melanoma          | 0.63                      | 2.55          | 0.27        | 0.66       | 1.54        | 4.56         | 1.77           | 1.35          | 0.94         | 3.9                      | 1                       | 0                          |
| UACC-62   | Melanoma          | 0.19                      | 0.68          | 0           | 1.51       | 0.54        | 10.01        | 0.64           | 1.12          | 0.67         | 0.6                      | 1.5                     | 0.8                        |
| IGROV-1   | Ovary             | 0.87                      | 1.45          | 0.76        | 0.43       | 0.48        | 2.66         | 2.66           | 0.79          | 1.18         | 0                        | 0.9                     | 1.2                        |
| OVCAR3    | Ovary             | 0.16                      | 0.41          | 2.47        | 0.16       | 0.54        | 0.23         | 1              | 0.38          | 1.06         | 0.3                      | 1.1                     | 1.6                        |
| OVCAR4    | Ovary             | 0.28                      | 2.19          | 1.03        | 0.39       | 0.64        | 0.56         | 0.95           | 0.46          | 1.04         | 0.4                      | 0.6                     | 1.3                        |
| OVCAR5    | Ovary             | 0.47                      | 1.38          | 2.46        | 0.46       | 0.54        | 0.67         | 0.63           | 1             | 2.61         | 0.3                      | 1.1                     | 1.6                        |
| OVCAR8    | Ovary             | 0.53                      | 1.67          | 1.77        | 0.25       | 1.06        | 0.78         | 0.6            | 1.23          | 0.85         | 0.6                      | 1.1                     | 1.2                        |
| SKOV-3    | Ovary             | 0.44                      | 1.96          | 1.46        | 0.26       | 0.73        | 0.95         | 0.53           | 0.28          | 1.15         | 0.6                      | 0.4                     | 0.4                        |
| DU-145    | Prostate          | 0.44                      | 1.16          | 1.54        | 0.27       | 0.93        | 1.98         | 0.81           | 0.64          | 0.99         | 0.8                      | 0                       | 1.2                        |
| PC3       | Prostate          | 4.25                      | 1.99          | 1.44        | 0.37       | 0.55        | 0.39         | 0.63           | 0.49          | 0.91         | 0.5                      | 0.6                     | 0.8                        |
| 786-O     | Renal             | 0.44                      | 2.2           | 0           | 0.51       | 0.57        | 1.28         | 0.45           | 1.02          | 0.91         | 0.3                      | 0.9                     | 0.5                        |
| A498      | Renal             | 0.56                      | 1.35          | 0.43        | 0.81       | 0.81        | 12.3         | 2.68           | 1.77          | 0.95         | 0.4                      | 1.3                     | 1.2                        |
| ACHN      | Renal             | 1.28                      | 3.86          | 2.33        | 1.13       | 0.64        | 5.19         | 1.97           | 1.76          | 1.43         | 3                        | 1.4                     | 0.9                        |
| CAKI-1    | Renal             | 0.38                      | 2.33          | 2.18        | 0.66       | 1.33        | 3.73         | 1.16           | 0.55          | 1.02         | 0.7                      | 0.9                     | 1.2                        |
| RXF-393   | Renal             | 0.55                      | 1.24          | 0.86        | 0.34       | 0.56        | 0.7          | 0.47           | 0.91          | 0.54         | 0.9                      | 0.8                     | 0.4                        |
| SN12C     | Renal             | 0.21                      | 1.03          | 1.53        | 0.32       | 0.27        | 0.16         | 1.22           | 0.31          | 0.7          | 0.2                      | 1.3                     | 1.4                        |
| TK10      | Renal             | 1.3                       | 3.45          | 0.75        | 1.06       | 1.14        | 6.32         | 0.73           | 0.82          | 2.42         | 3.5                      | 1.2                     | 0.9                        |
| UO31      | Renal             | 0.91                      | 2.13          | 1.67        | 1.49       | 0.8         | 7.55         | 0.87           | 0.93          | 1.48         | 0.9                      | 1.3                     | 1.2                        |

<sup>a</sup> Tissue of origin.

<sup>b</sup> Numbers are basal expression levels relative to levels in BT549.

<sup>c</sup> Numbers are basal expression levels relative to levels in MDA-N.

<sup>d</sup> Basal protein expression relative to levels in BT549.

<sup>e</sup> CNS, central nervous system.

relative to the levels in MDA-N. Although some transcripts were more variable than others, in most cases variation was less than 10-fold across the NCI-ACDS.

The basal transcript levels in a subset of the lines were rechecked by comparing the RNA samples from the original isolation side by side with newly isolated RNA from freshly grown cells. Cell lines representing both the median and the most extreme expression levels were chosen for each probe. The values of the repeated measurements agreed well with the original values, showing only slight variations (Fig. 1).

For a number of the transcripts measured in this study, previous measurements of relative protein levels were available in the NCI-ACDS database. Comparison of our quantitation of basal mRNA levels with these protein data sets (Table 1) gives an additional indication of the robust nature of our measurements. As might be expected, there is a strong positive correlation between these two measurements where relative protein levels are available for comparison (BAX:  $r = 0.41$ ,  $P = 0.001$ ; BCL-X<sub>L</sub>:  $r = 0.55$ ,  $P = 0.000006$ ). These mRNA and protein level measurements are in good agreement, but there is also substantial variation in the protein level that is not explained by the mRNA measurements. Some of this unexplained variation may be attributable to posttranslational protein regulation, whereas some may reflect the different sources of error in the very different quantitation techniques necessarily used and the inherent difficulties in normalizing relative protein content. Although mRNA levels may not be a direct substitute for protein measurements, they can nonetheless be of predictive value.

#### Correlations between Basal RNA Levels of Different Genes.

We first looked for correlations between the basal mRNA levels of the 10 genes measured in the cell lines of the NCI-ACDS. The strongest correlation between these targets is for *CIP1/WAF1* and *BAX* (Fig. 2;  $r = 0.687$ ;  $P = 0.0001$ ). *CIP1/WAF1* basal levels also correlated well with the basal levels of *GADD45* ( $r = 0.471$ ;  $P = 0.0001$ ), a gene similarly regulated during cell growth arrest and stress responses (27). This may suggest that when both of these genes are expressed in a cell, they tend to maintain a relatively constant ratio with respect to each other. Previous experiments had suggested a compensatory mechanism whereby under stress conditions, a cell could offset a lack of *GADD45* induction with an unusually prolonged and large magnitude *CIP1/WAF1* response (7). Because the basal levels of these two genes correlate positively with each other rather than negatively, such compensation would appear to be engaged only during stress response, however, not during normal growth. The basal levels of the

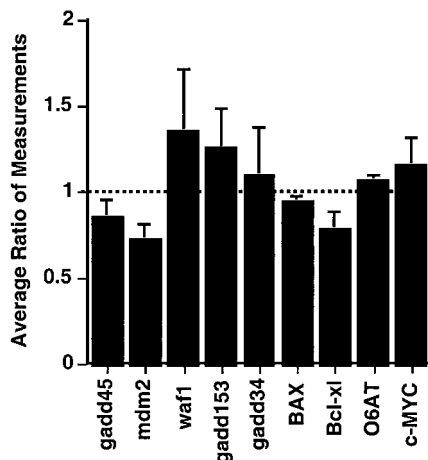


Fig. 1. Reproducibility of measurements. Bars, average ratio of repeated determinations of the expression level of the genes measured in three or more independently grown cultures of untreated, exponentially growing Molt4, CCRF-CEM, SKOV3, T47D, UACC62, HCT116, RKO, and NCI-H226. Error bars, SE.

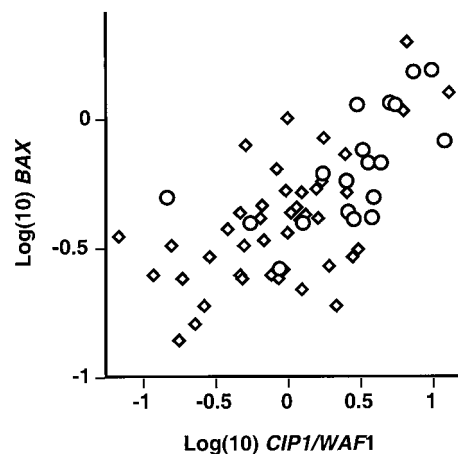


Fig. 2. Scatter plot showing the relative expression levels of *BAX* and *CIP1/WAF1* in each of the cell lines in the NCI-ACDS with wild-type (○) and mutant (◇) p53 function as previously determined (9).

three major *GADD* genes as measured here also correlate with each other (*GADD45* and *GADD153*:  $r = 0.36$ ;  $P = 0.004$ ; *GADD45* and *GADD34*:  $r = 0.42$ ;  $P = 0.0007$ ; *GADD153* and *GADD34*:  $r = 0.52$ ;  $P < 0.00005$ ), suggesting coordinate regulation of these genes under normal growth conditions and during stress response (12).

Despite reports that both basal (28) and stress-induced levels (29) of the *GADD* genes are down-regulated by overexpression of *c-Myc*, basal levels of the *GADD* genes do not correlate well with endogenous *c-MYC* mRNA levels ( $r = 0.13$ ;  $P > 0.25$ ). This may indicate that for *Myc*, mRNA is not a good predictor of protein levels or that additional regulators of the *GADD* genes may be more important in determining basal levels of these genes during exponential cell growth. It should also be noted that the previously reported down-regulation of the *gadd* genes by *c-Myc* occurred only in the presence of *Myc* overexpression, so it is possible that the effect of *c-Myc* levels on *gadd* gene regulation is not significant within the normal endogenous range of *c-MYC* expression.

**Relationship of Basal RNA Levels to p53 Status.** The most significant relationship between p53 status and any of the basal mRNA levels measured here was for *CIP1/WAF1* ( $P = 0.002$ ; Fig. 3A). Induction of *CIP1/WAF1* by ionizing radiation previously has been shown to be dependent on wild-type p53 function (30, 31). p53 may also play an important role in the basal regulation of *CIP1/WAF1*, because among p53 mutant cell lines, basal expression was extremely low in most cases. Basal levels of *BAX*, another gene with p53-regulated stress response (32, 33), also tended to be higher among p53 wild-type cell lines ( $P = 0.003$ ; Fig. 3B). Interestingly, no significant correlation was found between p53 status and basal levels of *GADD45*, despite the dependence of ionizing radiation induction of this gene on wild-type p53 function (34, 35) and the positive correlation of basal levels of *GADD45* with those of *CIP1/WAF1*. Induction of *GADD45* by other DNA-damaging stresses, such as UV radiation or alkylating agents, is regulated by both p53-dependent and -independent pathways (34, 36). The present results perhaps suggest a greater role for p53-independent mechanisms in maintenance of basal *GADD45* levels.

**Induced Responses Do Not Compensate for Differences in Basal Levels.** The role of genes such as *GADD45*, *CIP1/WAF1*, and *MDM2* in stress response has been well characterized both in our laboratory and others (18, 20, 37, 38), and the ionizing radiation response of all three genes has been found to be dependent on wild-type p53. Although in this study the basal level of only *BAX* and *CIP1/WAF1* correlated with p53 status, we were interested to see if there was a

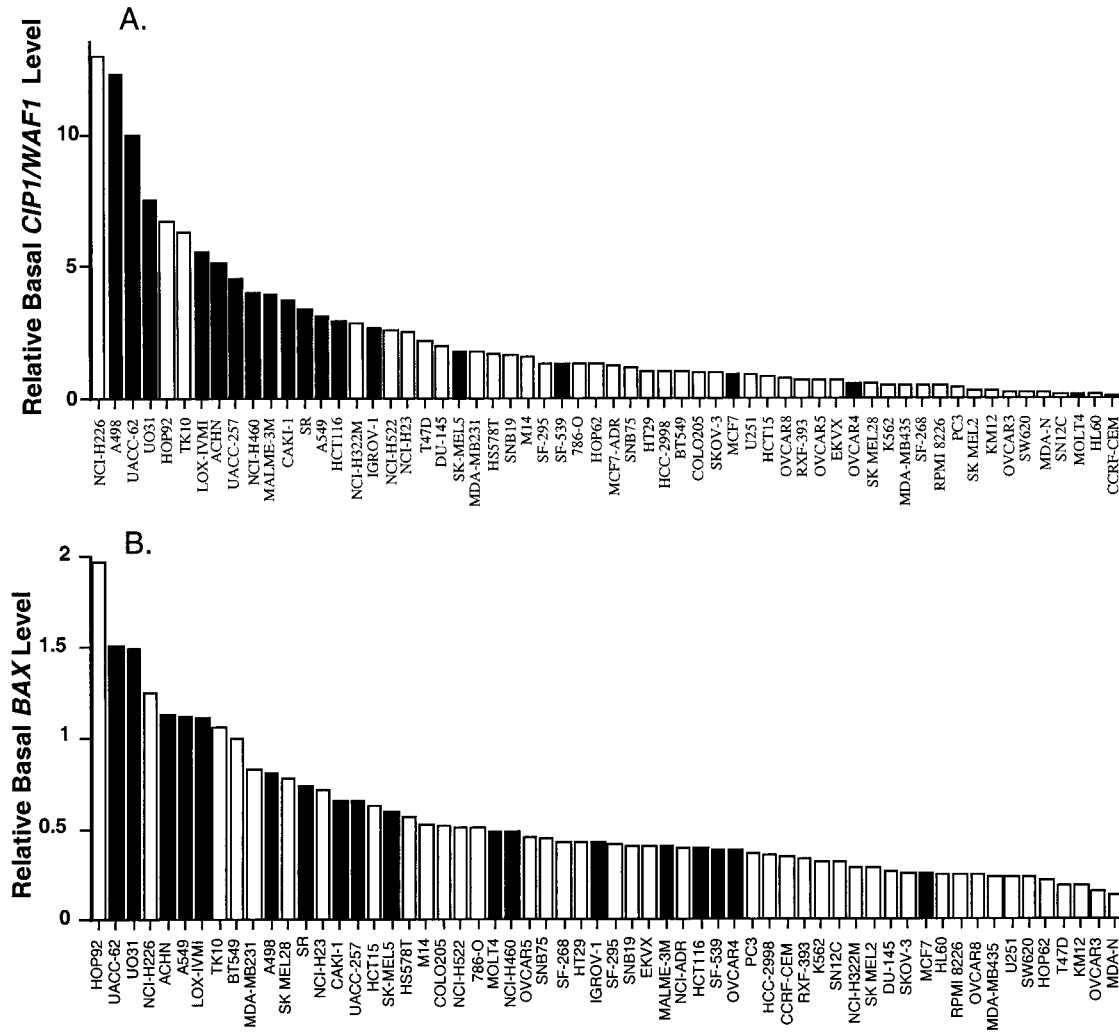


Fig. 3. A, ranked order of relative expression levels of *CIP1/WAF1* mRNA in exponentially growing, untreated cells. ■, cell lines with wild-type p53; □, cell lines with mutant p53. B, ranked order of relative expression levels of *BAX* mRNA in exponentially growing, untreated cells. ■, cell lines with wild-type p53; □, cell lines with mutant p53.

relationship between basal levels and ionizing radiation induction of these genes or if induction raised the absolute expression to similar levels in all of the cell lines, irrespective of basal levels. The relative induction of mRNA by  $\gamma$ -rays was measured previously for these three genes in the 60 cell lines of the NCI-ACDS (9). Comparing the basal levels of these genes with their absolute induced levels (the product of the basal level and the relative fold-induction in each line) there is a trend of increased absolute induced levels with increasing

basal expression both within the p53 wild-type subset of cell lines (Fig. 4) and across the entire NCI-ACDS panel (*GADD45*:  $r = 0.71$ ; *CIP1/WAF1*:  $r = 0.63$ ; *MDM2*:  $r = 0.94$ ; all  $P < 0.00005$ ), despite the relative lack of induction in the p53 mutant cell lines. This indicates that the stress response of these genes does not compensate for their variations in basal expression. Rather, the relative basal expression levels of these genes are an important determinant of absolute stress-induced expression levels, regardless of the fold-

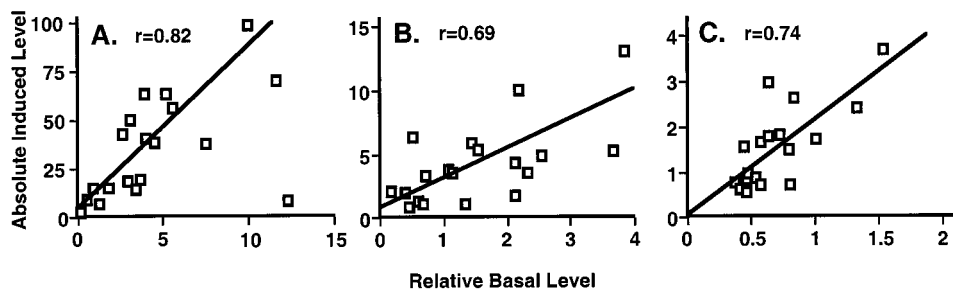


Fig. 4. A, relationship between the relative basal level of *CIP1/WAF1* mRNA expression in growing, untreated cells and the absolute ionizing radiation-induced level [defined as the relative basal level multiplied by the overall fold induction 4 h after treatment with 20 Gy  $\gamma$ -rays (9)] in the p53 wild-type cell lines of the NCI-ACDS. B, relationship between the relative basal level of *GADD45* mRNA expression in growing, untreated cells and the absolute ionizing radiation-induced level in the p53 wild-type cell lines of the NCI-ACDS. C, relationship between the relative basal level of *MDM2* mRNA expression in growing, untreated cells and the absolute ionizing radiation-induced level in the p53 wild-type cell lines of the NCI-ACDS.  $r$ , coefficient of correlation the p53 wild-type subset (A–C).

Table 2 Mechanisms of action of the standard set of anticancer agents included in the NCI-ADS

| Mechanistic class <sup>a</sup>   | Examples of agents  |
|----------------------------------|---|
| Alkylating agents (35)           | Mitomycin-C, CCNU, <sup>b</sup> PCNU, BCNU, carboplatin, <i>cis</i> -platinum |
| DNA antimetabolites (16)         | Thioguanine, Ara-C, 5-FUdR, hydroxyurea, 5-aza-2'-deoxycytidine               |
| RNA/DNA antimetabolites (19)     | Methotrexate, antifolates, 5-azacytidine, 5-fluorouracil                      |
| Topoisomerase I inhibitors (24)  | Camptothecin and its derivatives  |
| Topoisomerase II inhibitors (16) | Daunomycin, Adriamycin, VP-16, m-AMSA   |
| Antimitotic agents (13)          | Colchicine, vinblastin, vincristin, Taxol                                     |

<sup>a</sup> Numbers in parentheses are the total number of agents in the class.

<sup>b</sup> CCNU, *N*-(2-chloroethyl)-*N'*-cyclohexyl-*N*-nitrosourea; BCNU, Bis (2-chloroethyl)nitrosourea; Ara-C, cytosine arabinoside; 5-FUdR, 5-fluoro-2'-deoxyuridine; VP-16, etoposide; m-AMSA, amsacrine.

induction in a particular cell line. The finding that the relative relationship of gene expression levels among the cell lines is similar before and after genotoxic stress, irrespective of p53 status, supports the use of basal expression level data as an informative marker for predicting genotoxic response.

**Correlations with Drug Sensitivities.** We next compared basal expression levels of the 10 genes quantitated here with sensitivity to a set of 122 standard chemotherapy agents in the NCI-ACDS (Table 2). Loss of detectable expression of O6AT at either the mRNA or protein level is estimated to occur in ~15–25% of primary human tumors (39), resulting in the Mer<sup>-</sup> phenotype. A slightly higher fraction, 18/60 (30%), of the cell lines in the NCI-ACDS panel expressed undetectable levels of O6AT in our study (Table 1). To test the ability of our gene expression measurements to identify mechanisms of drug action, we first examined the correlation of Mer<sup>+</sup>/Mer<sup>-</sup> phenotype with activity of O<sup>6</sup>-alkylating agents ( $r = -0.44$ ;  $P < 0.05$ ). This contrasted with the lack of correlation between the Mer phenotype and toxicity of other alkylators ( $r = -0.04$ ). This would be expected because the O6AT DNA repair protein is specific for the reversal of the O<sup>6</sup> lesions generated by these agents but is not active against other lesions or other mechanisms of toxicity (Fig. 5A and B). As a specific example, a comparison of the GI<sub>50</sub> values for PCNU, one of the agents in this mechanistic class, is illustrated in Fig. 5C for cell lines expressing (Mer<sup>+</sup>) or not expressing (Mer<sup>-</sup>) O6AT. Expression of O6AT has previously been shown to be a good predictor of sensitivity of a cell line to nitrosourea compounds such as this (39). These results provide a positive control illustrating the identification of drugs by mechanism of action through informatic analysis of RNA expression data and provide a validation of the methodology used here.

One of the most striking findings in this analysis is a broad negative correlation ( $r = -0.3$ ) between basal *BCL-X<sub>L</sub>* levels and overall drug sensitivity to all of the categories of drugs tested, with the exception of one subgroup, which includes antimetabolites such as thioguanine, thiopurine, and 5-azacytidine (Fig. 6A). This pattern is almost an exact mirror image of the pattern of drug sensitivities correlated with p53 status (Fig. 6B; an overall positive correlation of ~0.23; Ref. 9). *Bcl-X<sub>L</sub>* is a member of the Bcl2 family of apoptosis-regulating proteins, which has been shown to protect against p53-mediated apoptosis (40, 41). An alternately spliced form of the same transcript codes for *Bcl-X<sub>S</sub>*, which antagonizes the activity of the major *Bcl-X<sub>L</sub>* protein to promote apoptosis (42), but this message is expressed at very low levels in most cell lines examined. Overexpression of *BCL-X* in murine lymphoid cells has been reported to have a protective effect against the toxicity of diverse agents including cyclosporin A, rapamycin, FK-506 (43), bleomycin, cisplatin, etoposide, vincristine, hygromycin B, mycophenolic acid (44), vinblastine, teniposide, methotrexate, fluorouracil, hydroxyurea, and  $\gamma$ -irradiation (45). Conversely, suppression of *Bcl-X<sub>L</sub>* levels in a human cancer cell line by use of either *BCL-X* antisense or overexpression of its antagonist Bak was found to sensitize the cells to apoptosis after treatment with 5-fluorouracil or cisplatin (46).

Although overexpression of Bcl2, another major antiapoptotic protein, has also been shown to protect against killing by many different agents (47, 48), the basal levels of *BCL2* mRNA in untreated cells show no correlation with overall sensitivity to the chemotherapy agents in this study (Fig. 6C), possibly indicating *Bcl-X<sub>L</sub>* as a more important regulator of cell death. In addition, levels of *BAX*, which codes for an apoptosis-promoting protein, do not show a comprehensive correlation with drug toxicity across the NCI-ACDS (Fig. 6D) as might have been expected. This may suggest that Bax-independent mechanisms of *Bcl-X<sub>L</sub>* action may play a predominant role in determining the survival of cancer cells exposed to chemotherapeutic agents. On the other hand, because only basal expression levels were measured here, we cannot exclude the possibility that drug-inducible levels of *BAX* or *BCL-2* may correlate with tumor cell line responses to anticancer compounds. The pattern of correlations between *BCL-X* basal expression and cytotoxicity does appear to be specific to expression of this gene, however, and not merely a general hallmark of apoptosis-regulating genes.

Because *BCL-X* previously had been shown to be induced by ionizing radiation in a small subset of cancer cell lines (49), we measured  $\gamma$ -ray induction of this gene in an additional 31 of the 60 cell lines (data not shown). We found a relationship between basal and absolute induced levels similar to ( $r = 0.79$ ;  $P < 0.0001$ ) that found for the previously measured genes *GADD45*, *CIP1/WAF1*, and *MDM2* discussed above, indicating that the relative relationship of *BCL-X* levels are also very similar before and after treatment. The relative inductions of *BCL-X* were furthermore not predictive of cytotoxicity in either the Standard set of 122 agents or the larger Unidrug set.<sup>8</sup>

Previous measurements of doubling time for the cell lines of the NCI-ACDS (9) also show a significant negative correlation across all of the drug classes examined (Fig. 6E). This indicates, as might be expected, general increased chemoresistance the more slowly a cell divides. This pattern was similar to that found for *BCL-X*, so it was possible that *BCL-X* expression levels were acting as a marker for cellular growth rate rather than chemosensitivity. The correlation between doubling time and *BCL-X* expression is not significant, however ( $P > 0.05$ ). Furthermore, examining the partial correlation of *BCL-X* levels and drug sensitivity by "removing" the statistical effect of doubling time still demonstrates a highly significant effect for *BCL-X* (Fig. 6F), indicating an effect independent of doubling time. Similarly, the protective effect of *BCL-X* also appears to be independent of p53 status because there was no difference in distribution of *BCL-X* levels among the p53 wild-type and p53 mutant cell lines in the NCI-ACDS. The significance of correlations between drug sensitivities and *BCL-X* expression was also unaffected by p53 status of the cell lines, as demonstrated by either partial correlation (Fig. 6G) or by the exclusion of the p53 wild-type cell lines in determining the drug sensitivity correlations (Fig. 6H).

<sup>8</sup> Details are available at <http://rex.nci.nih.gov/RESEARCH/basic/lbc/fomace.html> and <http://www.chemodb.org>.

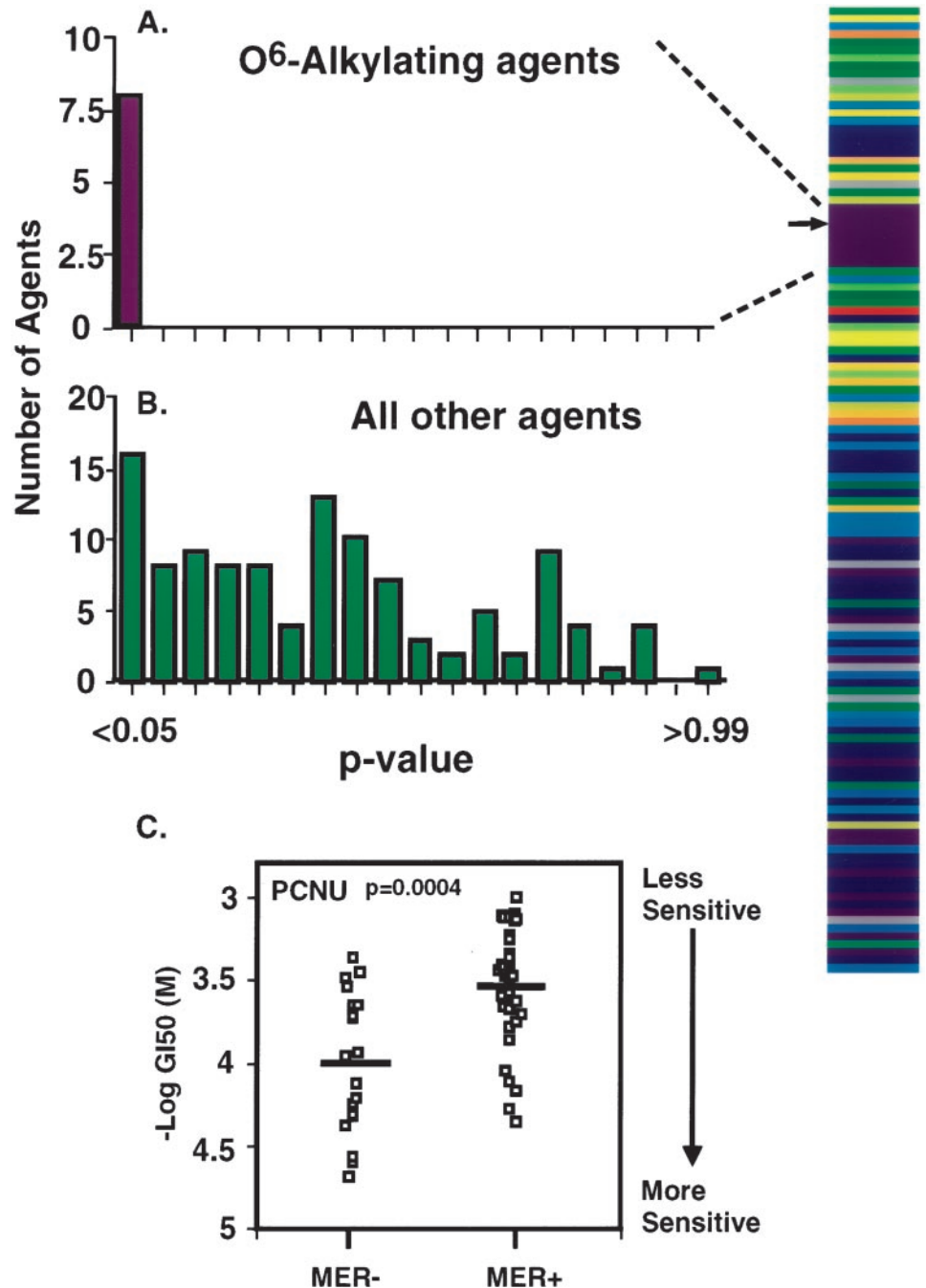


Fig. 5. A, plot of  $P$  for the significance of correlations between the toxicity of  $O^6$ -alkylating agents and the binary expression of O6AT in the cell lines of the NCI-ACDS. First column of the histogram:  $P < 0.05$  indicates a significant negative correlation between gene expression and toxicity or a protective effect of gene expression; dashed lines: location of the nitrosourea subgroup of the alkylating agents in the overall  $P$  matrix for O6AT (right of the histograms). Agents with similar mechanisms are grouped together, and a dark purple block represents those with significant negative correlations with O6AT expression. (The color key for the entire  $P$  spectrum is shown in Fig. 6). B, plot of the  $P$  for the agents tested that act via mechanisms other than  $O^6$ -alkylation. Although some of these agents show a significant negative correlation with O6AT expression, the  $P$  matrix to the right reveals that these significant values are scattered, not clustered within one mechanism of action, as in the case of the nitrosoureas shown in A. C, relationship between O6AT expression and sensitivity of the cell lines in the NCI-ACDS to a representative nitrosourea compound indicated by the arrow in the  $P$  matrix: PCNU (CAS 13909029). The cell lines have been divided into two groups: Mer+ (those expressing measurable levels of O6AT) and Mer- (those not expressing detectable levels of O6AT). □, each point represents the sensitivity of an individual cell line expressed as  $GI_{50}$ ; bars, median for each category. A  $-\log(GI_{50})$  value of 4 corresponds to a concentration of  $10^{-4}$  M.

## DISCUSSION

The NCI-ACDS screen for drug activity, the associated molecular target databases, and correlation analysis tools make a potent combination to identify markers associated with chemoresistance and other parameters relevant to cancer treatment. The novel factor analysis described here, which uses partial correlations to remove potential confounding effects of previously described sensitivity factors, increases the utility of this approach. We have used these analyses to find correlations between the parameters in the NCI-ACDS database and the basal expression of 10 genes involved in the cellular response to stress. Although many interesting relationships were uncovered, the most striking was the overall protective effect found for expression of  $BCL-X_L$ .

It is interesting that the protective effect of  $Bcl-X_L$  extends across

all of the cancer cell types in the NCI-ACDS panel and is not restricted to lymphoid and myeloid cell lines, which are especially prone to undergo apoptosis.  $BCL-X_L$  induction by ionizing radiation previously has been shown to occur primarily in cell lines with both wild-type p53 function and a propensity to undergo rapid radiation-induced apoptosis (49). In contrast to the specificity of cell type required for  $BCL-X$  induction, the protective effect of high basal levels of  $BCL-X$  extends across the NCI-ACDS, depending neither on wild-type p53 function, nor on cell type. In a smaller set of cell lines, relatively low basal levels of  $BCL-X_L$  have been shown to correlate with a greater degree of  $\gamma$ -ray-induced apoptosis (49), suggesting the protective effect of high basal levels may extend also to ionizing radiation. Although no quantitative measurement of radiation-induced apoptosis has been made for the 60 cell lines of the NCI-ACDS, a

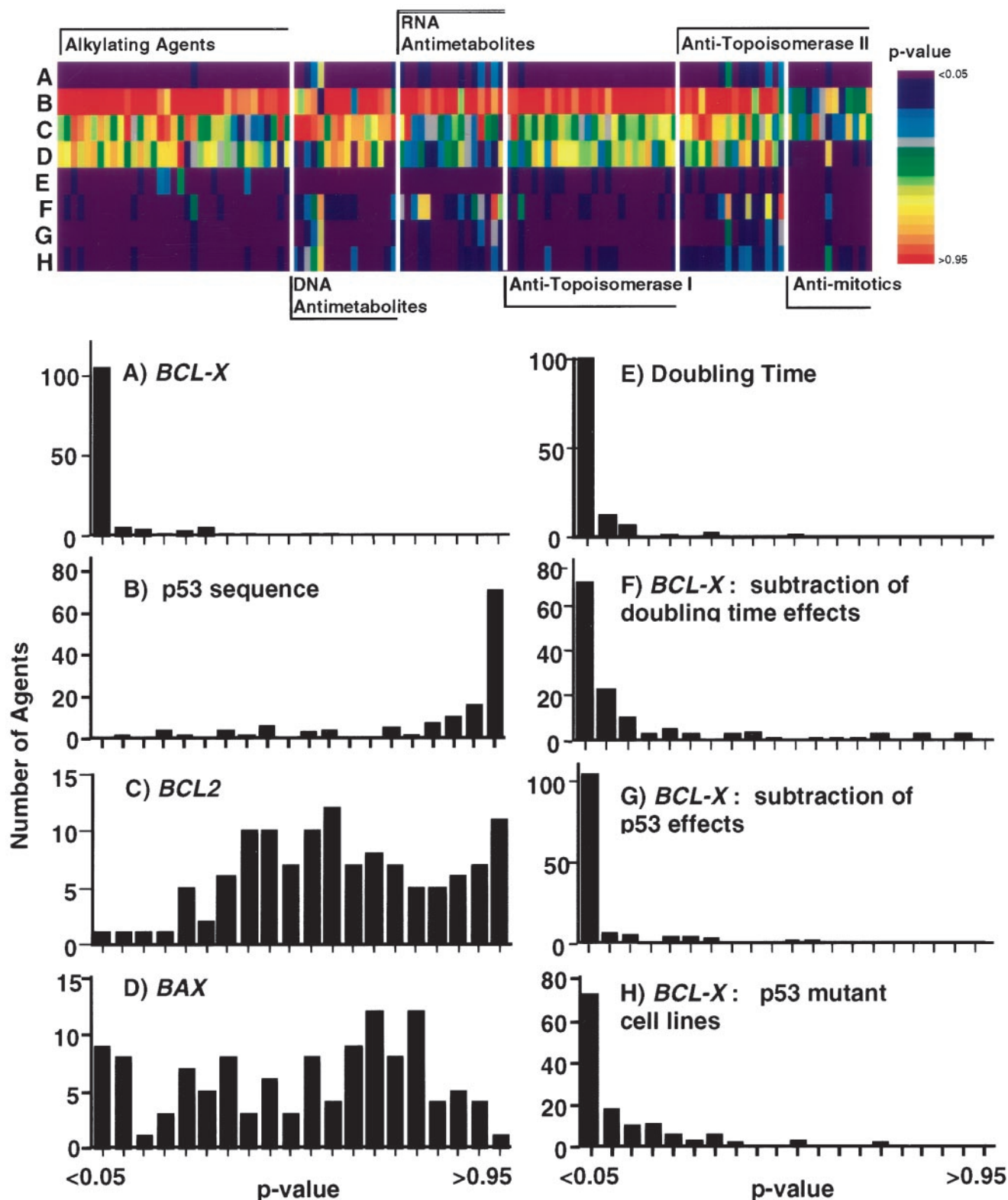


Fig. 6. Histograms and Spearman  $P$  matrix relating the activity of the set of 122 standard chemotherapy agents to expression levels of *BCL-X* and other genes with known roles in apoptosis. The values have been color coded according to the scale shown. Values  $< 0.05$  indicate a significant negative correlation (protective effect of gene expression), whereas values  $> 0.95$  indicate a significant positive correlation (sensitizing effect of gene expression). The proposed major mechanism of action of each group of compounds is shown along the borders of the matrix (the term “alkylating agents” is used broadly to include platinating agents). Each column within the matrix represents the significance of correlation between gene expression and toxicity of an individual drug within the mechanistic classes. Histograms show the distribution of  $P$  for correlations with relative levels of *BCL-X* expression (A), binary p53 status (Pearson  $P$ ; B), *BCL2* expression (C), *BAX* expression (D), and cell generation time (E), as determined by population doubling time. The distribution of  $P$  associated with correlations of drug sensitivities with expression of *BCL-X* after correction for contributions of doubling time (F) or p53 status of the cells (G) are also shown.  $P$  for correlation of drug sensitivities and *BCL-X* expression among only the p53 mutant cell lines (H). Comparisons of the rows in the  $P$  matrix with the corresponding histogram show the distribution of significant associations among the various mechanistic classes.

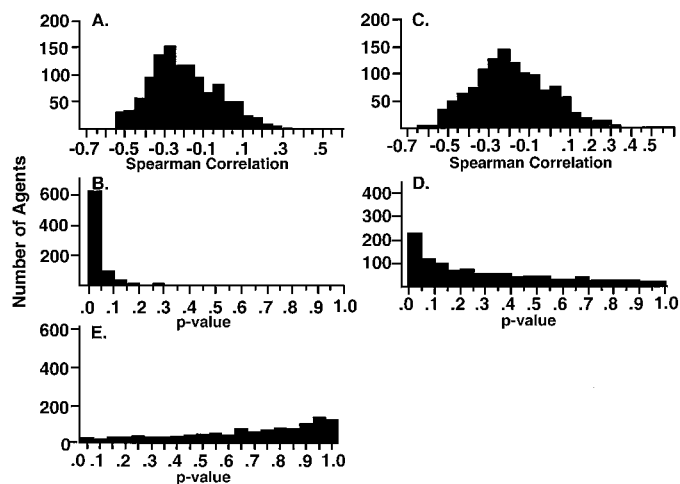


Fig. 7. *A*, distribution of Spearman correlations between *BCL-X* mRNA expression and sensitivity to a larger set of 1247 drugs with more diverse mechanisms of action; *B*, the associated *P* indicating the significance of the correlations. *C*, distribution of Spearman correlations between *BCL-X*<sub>L</sub> protein expression levels and sensitivity to the Unidrug 1247, and *D*, their associated *P*. High levels of *BCL-X* expression appear to be broadly protective against a great diversity of chemotoxic agents. *E*, distribution of *P* for the Pearson correlations between p53 wild-type status and sensitivity to the Unidrug set of 1247 agents. Compare the shape of this distribution with that for the smaller set of 122 standard chemotherapy agents seen in Fig. 6*B*.

comparison of the basal *BCL-X* levels in the lymphoid/myeloid panel (lines very prone to apoptosis; mean,  $0.34 \pm 0.10$ ) with levels in all of the other cell lines (mean,  $0.93 \pm 0.08$ ) indicates a similar trend. This implies that basal levels of *BCL-X* can play a major role in the determination of cellular response to a wide variety of chemotherapeutic agents, perhaps through modulation of apoptosis.

Unlike the sensitizing effect on cell killing previously seen for wild-type p53 (9), the protective effect of *BCL-X* extends beyond the more classical cancer therapeutics. This is illustrated with the “Unidrug 1247,” a set of 1247 agents from the NCI-ACDS database having maximally diverse activity patterns, and in theory, 1247 distinguishable biochemical mechanisms of cell killing.<sup>6</sup> Although the dependence of toxicity on p53 status is no longer evident in this larger survey of agents, the (inverse) association between toxicity and *BCL-X* expression (Fig. 7, *A* and *B*) remains essentially unchanged from that seen across the smaller set of drug mechanisms. A similar pattern of correlations is also observed between drug activity and measurements of *Bcl-X*<sub>L</sub> protein expression (Fig. 7, *C* and *D*). A  $\chi^2$  comparison of the drug activity patterns in the Unidrug 1247 for *Bcl-X*<sub>L</sub> measured as mRNA versus protein had a  $P < 0.0001$ , again indicating good agreement between the two measurements. In contrast, comparison between *BAX* expression at either the mRNA or protein level and sensitivity to this larger drug set shows no pattern of overall correlation (data not shown), consistent with the results in the initial set of 122 agents (Fig. 6*C*). Unlike the case with *BCL-X*, when the bias introduced by multiple drugs sharing a small number of cytotoxic mechanisms is removed by considering the diverse mechanisms included in the Unidrug set, the strongly significant dependence of drug toxicity on wild-type p53 status (as seen in Fig. 6*B*) is no longer strikingly apparent (Fig. 7*E*), indicating that the protective effect of *BCL-X* expression may be much broader than the sensitization by wild-type p53.

The broad nature of the association between endogenous *BCL-X* expression and protection from chemotoxicity implicates this gene as an extremely important general determinant of cell death and suggests a p53-independent mechanism of *Bcl-X*<sub>L</sub> action as a major component of chemoresistance in cancer cells. In addition, the lack of dependence on wild-type p53 function increases the attractiveness of *Bcl-X*<sub>L</sub> as a

potential target of cancer therapy, because the majority of human cancers have lost p53 function (50, 51). Such p53-mutant tumors are generally more refractory to chemotherapy, as reflected in the increased chemoresistance of cell lines with aberrant p53 (9). A therapeutic approach targeting *Bcl-X*<sub>L</sub> may be able to circumvent the protective effect conferred by loss of normal p53 function in many tumors.

## ACKNOWLEDGMENTS

We thank Edward A. Sausville for his contributions to the NCI-ACDS database.

## REFERENCES

- Monks, A., Scudiero, D., Skehan, P., Shoemaker, R., Paull, K., Vistica, D., Hose, C., Langley, J., Cronise, P., Vaigro-Wolff, A., *et al.* Feasibility of a high-flux anticancer drug screen using a diverse panel of cultured human tumor cell lines. *J. Natl. Cancer Inst.*, **83**: 757–766, 1991.
- Grever, M. R., Schepartz, S. A., and Chabner, B. A. The National Cancer Institute: cancer drug discovery and development program. *Semin. Oncol.*, **19**: 622–638, 1992.
- Weinstein, J. N., Myers, T. G., O'Connor, P. M., Friend, S. H., Fornace, A. J., Jr., Kohn, K. W., Fojo, T., Bates, S. E., Rubinstein, L. V., Anderson, N. L., Buolamwini, J. K., Osdol, W. W., Monks, A. P., Scudiero, D. A., Sausville, E. A., Zaharevitz, D. W., Bunow, B., Johnson, G. S., Wittes, R. E., and Paull, K. D. An information intensive approach to the molecular pharmacology of cancer. *Science (Washington DC)*, **275**: 343–349, 1997.
- Myers, T. G., Anderson, N. L., Waltham, M., Li, G., Buolamwini, J. K., Scudiero, D. A., Paull, K. D., Sausville, E. A., and Weinstein, J. N. A protein expression database for the molecular pharmacology of cancer. *Electrophoresis*, **18**: 647–653, 1997.
- Amundson, S. A., Bittner, M., Chen, Y. D., Trent, J., Meltzer, P., and Fornace, A. J., Jr. cDNA microarray hybridization reveals complexity and heterogeneity of cellular genotoxic stress responses. *Oncogene*, **18**: 3666–3672, 1999.
- DeRisi, J., Penland, L., Brown, P. O., Bittner, M. L., Meltzer, P. S., Ray, M., Chen, Y., Su, Y. A., and Trent, J. M. Use of a cDNA microarray to analyse gene expression patterns in human cancer. *Nat. Genet.*, **14**: 457–460, 1996.
- Bae, I., Smith, M. L., Sheikh, M. S., Zhan, Q., Scudiero, D. A., Friend, S. H., O'Connor, P. M., and Fornace, A. J., Jr. An abnormality in the p53 pathway following  $\gamma$ -irradiation in many wild-type p53 human melanoma lines. *Cancer Res.*, **56**: 840–847, 1996.
- Carrier, F., Georgel, P. T., Pourquier, P., Blake, M., Kontny, H. U., Antinore, M. J., Gariboldi, M., Myers, T. G., Weinstein, J., Pommier, Y., and Fornace, A. J., Jr. Gadd45, a p53-responsive stress protein, modifies DNA accessibility on damaged chromatin. *Mol. Cell. Biol.*, **19**: 1673–1685, 1999.
- O'Connor, P. M., Jackman, J., Bae, I., Myers, T. G., Fan, S., Mutoh, M., Scudiero, D., Monks, A., Sausville, E. A., Weinstein, J. N., Friend, S., Fornace, A. J., Jr., and Kohn, K. W. Characterization of the p53 tumor suppressor pathway in cell lines of the National Cancer Institute anticancer drug screen and correlations with the growth-inhibitory potency of 123 anticancer agents. *Cancer Res.*, **57**: 4285–4300, 1997.
- Chomczynski, P., and Sacchi, N. Single-step method of RNA isolation by acid guanidinium thiocyanate-phenol-chloroform extraction. *Anal. Biochem.*, **162**: 156–159, 1987.
- Hollander, M. C., and Fornace, A. J., Jr. Estimation of relative mRNA content by filter hybridization to a polythymidylate probe. *Biotechniques*, **9**: 174–179, 1990.
- Jackman, J., Alamo, I., and Fornace, A. J., Jr. Genotoxic stress confers preferential and coordinate mRNA stability on the five *gadd* genes. *Cancer Res.*, **54**: 5656–5662, 1994.
- Luethy, J. D., Fargnoli, J., Park, J. S., Fornace, A. J., Jr., and Holbrook, N. J. Isolation and characterization of the hamster *gadd153* gene. Activation of promoter activity by agents that damage DNA. *J. Biol. Chem.*, **265**: 16521–16526, 1990.
- Koch-Paiz, C. A., Momenan, R., Amundson, S. A., Lamoreaux, E., and Fornace, A. J., Jr. Estimation of relative mRNA content by filter hybridization to a polyuridylic probe. *Biotechniques*, **29**: 706–714, 2000.
- Kitada, S., Andersen, J., Akar, S., Zapata, J. M., Takayama, S., Krajewski, S., Wang, H. G., Zhang, X., Bullrich, F., Croce, C. M., Rai, K., Hines, J., and Reed, J. C. Expression of apoptosis-regulating proteins in chronic lymphocytic leukemia: correlations with *in vitro* and *in vivo* chemoresponses. *Blood*, **91**: 3379–3389, 1998.
- Fornace, A. J., Jr., Nebert, D. W., Hollander, M. C., Luethy, J. D., Papathanasiou, M., Fargnoli, J., and Holbrook, N. J. Mammalian genes coordinately regulated by growth arrest signals and DNA-damaging agents. *Mol. Cell. Biol.*, **9**: 4196–4203, 1989.
- Fornace, A. J., Jr., Jackman, J., Hollander, M. C., Hoffman-Liebermann, B., and Liebermann, D. A. Genotoxic-stress-response genes and growth-arrest genes; the *gadd*, *MyD*, and other genes induced by treatments eliciting growth arrest. *Ann. NY Acad. Sci.*, **663**: 139–153, 1992.
- Zhan, Q., Carrier, F., and Fornace, A. J., Jr. Induction of cellular p53 activity by DNA-damaging agents and growth arrest. *Mol. Cell. Biol.*, **13**: 4242–4250, 1993.
- Zhang, W., Grasso, L., McClain, C. D., Gambel, A. M., Cha, Y., Travali, S., Deisseroth, A. B., and Mercer, W. E. p53-independent induction of *WAF1/CIP1* in human leukemia cells is correlated with growth arrest accompanying monocyte/macrophage differentiation. *Cancer Res.*, **55**: 668–674, 1995.

20. Smith, M. L., and Fornace, A. J., Jr., Mammalian DNA damage-inducible genes associated with growth arrest and apoptosis. *Mutat. Res.*, *340*: 109–124, 1996.
21. Fornace, A. J., Jr., Alamo, I. J., Hollander, M. C., and Lamoreaux, E. Induction of heat shock protein transcripts and B2 transcripts by various stresses in Chinese hamster cells. *Exp. Cell Res.*, *182*: 61–74, 1989.
22. Fornace, A. J., Jr., Alamo, I. J., Hollander, M. C., and Lamoreaux, E. Ubiquitin mRNA is a major stress-induced transcript in mammalian cells. *Nucleic Acids Res.*, *17*: 1215–1230, 1989.
23. Fornace, A. J., Jr., Alamo, I. J., and Hollander, M. C. DNA damage-inducible transcripts in mammalian cells. *Proc. Natl. Acad. Sci. USA*, *85*: 8800–8804, 1988.
24. Kafatos, F. C., Jones, C. W., and Efstratiadis, A. Determination of nucleic acid sequence homologies and relative concentrations by a dot hybridization procedure. *Nucleic Acids Res.*, *7*: 1542–1552, 1979.
25. Hollander, M. C., and Fornace, A. J., Jr., Induction of *fos* RNA by DNA-damaging agents. *Cancer Res.*, *49*: 1687–1692, 1989.
26. Zhan, Q., Bae, I., Kastan, M. B., and Fornace, A. J., Jr., The p53-dependent  $\gamma$ -ray response of *GADD45*. *Cancer Res.*, *54*: 2755–2760, 1994.
27. Zhan, Q., El-Deiry, W., Bae, I., Alamo, I., Jr., Kastan, M. B., Vogelstein, B., and Fornace, A. J., Jr., Similarity of the DNA-damage responsiveness and growth-suppressive properties of *WAF1* to *GADD45*. *Int. J. Oncol.*, *6*: 937–946, 1995.
28. Marhin, W. W., Chen, S., Facchini, L. M., Fornace, A. J., Jr., and Penn, L. Z. Myc represses the growth arrest gene *gadd45*. *Oncogene*, *14*: 2825–2834, 1997.
29. Amundson, S. A., Zhan, Q., Penn, L. Z., and Fornace, A. J., Jr., Myc suppresses induction of the growth arrest genes *gadd34*, *gadd45* and *gadd153* by DNA-damaging agents. *Oncogene*, *17*: 2149–2154, 1998.
30. El-Deiry, W. S., Tokino, T., Velculescu, V. E., Levy, D. B., Parsons, R., Trent, J. M., Lin, D., Mercer, W. E., Kinzler, K. W., and Vogelstein, B. WAF1, a potential mediator of p53 tumor suppression. *Cell*, *75*: 817–825, 1993.
31. El-Deiry, W. S., Harper, J. W., O'Connor, P. M., Velculescu, V. E., Canman, C. E., Jackman, J., Pietenpol, J. A., Burrell, M., Hill, D. E., Wang, Y., *et al.* WAF1/CIP1 is induced in p53-mediated G<sub>1</sub> arrest and apoptosis. *Cancer Res.*, *54*: 1169–1174, 1994.
32. Miyashita, T., Krajewski, S., Krajewska, M., Wang, H. G., Lin, H. K., Liebermann, D. A., Hoffman, B., and Reed, J. C. Tumor suppressor p53 is a regulator of *bcl-2* and *bax* gene expression *in vitro* and *in vivo*. *Oncogene*, *9*: 1799–1805, 1994.
33. Zhan, Q., Fan, S., Bae, I., Guillouf, C., Liebermann, D. A., O'Connor, P. M., and Fornace, A. J., Jr. Induction of *BAX* by genotoxic stress in human cells correlates with normal p53 status and apoptosis. *Oncogene*, *9*: 3743–3751, 1994.
34. Kastan, M. B., Zhan, Q., El-Deiry, W. S., Carrier, F., Jacks, T., Walsh, W. V., Plunkett, B. S., Vogelstein, B., and Fornace, A. J., Jr. A mammalian cell cycle checkpoint utilizing p53 and *GADD45* is defective in ataxia telangiectasia. *Cell*, *71*: 587–597, 1992.
35. Hollander, M. C., Alamo, I., Jackman, J., McBride, O. W., and Fornace, A. J., Jr. Sequence conservation and DNA damage-responsiveness of the mammalian *gadd45* gene. *J. Biol. Chem.*, *268*: 24385–24393, 1993.
36. Zhan, Q., Fan, S., Smith, M. L., Bae, I., Yu, K., Alamo, Jr, I., O'Connor, P. M., and Fornace, A. J., Jr. Abrogation of p53 function affects the response of *gadd* genes to DNA base damaging agents and medium starvation. *DNA Cell Biol.*, *15*: 805–815, 1996.
37. Ko, L. J., and Prives, C. p53: puzzle and paradigm. *Genes Dev.*, *10*: 1054–1072, 1996.
38. Gorospe, M., Martindale, J. L., Sheikh, M. S., Fornace, A. J., Jr., and Holbrook, N. J. Regulation of *p21<sup>CIP1/WAF1</sup>* expression by cellular stress: p53-dependent and p53-independent mechanisms. *Mol. Cell. Differ.*, *4*: 47–65, 1996.
39. Pegg, A. E., and Byers, T. L. Repair of DNA containing O<sup>6</sup>-alkylguanine. *FASEB J.*, *6*: 2302–2310, 1992.
40. Schott, A. F., Apel, I. J., Nunez, G., and Clarke, M. F. Bcl-X<sub>L</sub> protects cancer cells from p53-mediated apoptosis. *Oncogene*, *11*: 1389–1394, 1995.
41. Cheng, M. H.-Y., Levine, B., Boise, L. H., Thompson, C. B., and Hardwick, J. M. Bax-independent inhibition of apoptosis by Bcl-X<sub>L</sub>. *Nature (Lond.)*, *379*: 554–556, 1996.
42. Minn, A. J., Boise, L. H., and Thompson, C. B. Expression of Bcl-x<sub>L</sub> and loss of p53 can cooperate to overcome a cell cycle checkpoint induced by mitotic spindle damage. *Genes Dev.*, *10*: 2621–2631, 1996.
43. Gottschalk, A. R., Boise, L. H., Thompson, C. B., and Quintans, J. Identification of immunosuppressant-induced apoptosis in a murine B-cell line and its prevention by bcl-x but not bcl-2. *Proc. Natl. Acad. Sci. USA*, *91*: 7350–7354, 1994.
44. Minn, A. J., Rudin, C. M., Boise, L. H., and Thompson, C. B. Expression of bcl-x<sub>L</sub> can confer a multidrug resistance phenotype. *Blood*, *86*: 1903–1910, 1995.
45. Simonian, P. L., Grillot, D. A., and Nunez, G. Bcl-2 and Bcl-X<sub>L</sub> can differentially block chemotherapy-induced cell death. *Blood*, *90*: 1208–1216, 1997.
46. Kondo, S., Shinomura, Y., Kanayama, S., Higashimoto, Y., Kiyohara, T., Zushi, S., Kitamura, S., Ueyama, H., and Matsuzawa, Y. Modulation of apoptosis by endogenous Bcl-x<sub>L</sub> expression in MKN-45 human gastric cancer cells. *Oncogene*, *17*: 2585–2591, 1998.
47. Selvakumaran, M., Lin, H. K., Sjin, R. T. T., Reed, J. C., Liebermann, D., and Hoffman, B. The novel primary response gene *MyD118* and proto-oncogenes *myb*, *myc*, and *bcl2* modulate TGF $\beta$ 1 induced apoptosis of myeloid leukemia cells. *Mol. Cell. Biol.*, *14*: 2352–2356, 1994.
48. Park, D. S., Stefanis, L., Yan, C. Y. I., Farinelli, S. E., and Greene, L. A. Ordering the cell death pathway. Differential effects of BCL2, an interleukin-1-converting enzyme family protease inhibitor, and other survival agents on JNK activation in serum/nerve growth factor-deprived PC12 cells. *J. Biol. Chem.*, *271*: 21898–21905, 1996.
49. Zhan, Q., Alamo, I., Jr., Yu, K., Boise, L. H., O'Connor, P. M., and Fornace, A. J., Jr., The apoptosis-associated  $\gamma$ -ray response of BCL-X<sub>L</sub> depends on normal p53 function. *Oncogene*, *13*: 2287–2293, 1996.
50. Levine, A. J., Momand, J., and Finlay, C. A. The p53 tumor suppressor gene. *Nature (Lond.)*, *351*: 453–456, 1991.
51. Hollstein, M., Sidransky, D., Vogelstein, B., and Harris, C. C. p53 mutations in human cancers. *Science (Washington DC)*, *253*: 49–53, 1991.